Received: 8 May 2023 | Accepted: 1 June 2023

DOI: 10.1002/maco.202313909

ARTICLE

Materials and Corrosion

Investigating the potential of casein as a sustainable material in inhibiting the corrosion of aluminum in hydrochloric acid

Taher Rabizadeh | **Amin Matin Javid** | **Marjaneh Kazemi** | **Nima Vahedian Khezerlou** | **Hosna Ghanbari**

Department of Materials Engineering, Faculty of Mechanical Engineering, University of Tabriz, Tabriz, Iran

Correspondence
Taher Rabizadeh, Department of Materials Engineering, Faculty of Mechanical Engineering, University of Tabriz, 51666-16471 Tabriz, Iran.
Email: t.rabizadeh@tabrizu.ac.ir

Funding information
University of Tabriz

Abstract

In this study, the efficiency of casein in inhibiting the corrosion of aluminum in 0.1 M HCl was evaluated. Based on the weight loss data, increasing the amount of casein in the electrolyte from 50 to 500 ppm at 298 K decreased the corrosion rate of aluminum, for instance, from 2.53 to 0.58 $g\,m^{-2}\,h^{-1}$. It was also demonstrated that with casein, the activation energy of the corrosion phenomenon increased (e.g., from 6.52 kJ/mol without casein to 27.54 kJ/mol with 500 ppm casein). The electrochemical polarization studies illustrated that in the presence of 500 ppm casein, the corrosion current density remarkably decreased from 63.09 to 6.1 $\mu A/cm^2$. This was compatible with the increase in the charge transfer resistance recorded by electrochemical impedance spectroscopy. Furthermore, the X-ray photoelectron spectroscopy and atomic force microscopy techniques confirmed the adsorption of casein on the working electrodes, which caused an enhancement in the surface quality of the specimens.

KEYWORDS

adsorption isotherm, casein, corrosion inhibitor, EIS, polarization

1 | INTRODUCTION

Aluminum with some unique features such as low weight-to-strength ratio, proper electrical and thermal conductivity, low density, and high malleability has widely been utilized in various industries.[1–3]

In addition, it is well-documented that the formation of a thin surface layer protects aluminum from further oxidation and corrosion. However, this oxide layer has amphoteric nature and dissolves in severe acidic or alkaline solutions.[4] For example, in oil, gas, and petrochemical industries where HCl is extensively utilized for pickling and/or etching, the corrosion of Al is commonly observed.[5] Therefore, it is a few years that close collaborative research between academia and industry has been developed and great attention has been paid to tackling this issue.

Although different methods have been suggested to hinder the corrosion of metallic facilities, the injection of some chemicals known as "corrosion inhibitors" into the system is the most efficient and convenient approach.[6] In this regard, a considerable amount of organic compounds has been synthesized among which those with the electronegative donor atoms (i.e., N, P, O, S) and/or π electrons in their molecular structure are the most efficient ones.[7,8] For instance, it has been documented that pyridine,[9] tetrazole,[10] and pyrazinamide[11] molecules can reduce the corrosion of Al in HCl even at the parts per million level.

Recently, it has been noticed that the disposal of hazardous chemicals (e.g., corrosion inhibitors, fungicides) has adverse effects on human health.[12] For example, hydrazine, which is a volatile deoxygenator, may cause liver steatosis.[13] The presence of about 24.5 μg/L 5,6-dimethyl-1H-benzotriazole in human urine samples has also been reported.[14]

To address these issues, it is a few years that producing high-efficient corrosion inhibitors originating from natural resources such as plant extracts has been a major focus of research activities.[15] It was observed that 0.9 g/L of a baicalin derivative inhibited the corrosion of Al in 1 M HCl by 95%.[16] In another research, the powders extracted from the dendrocalamus brandisii leaves properly hindered the corrosion of the aluminum working electrodes in an HCl electrolyte.[17] *Cola nitida*[18] and *Thymus algeriensis*[19] extracts could also reduce the weight loss of aluminum in HCl.

Moreover, recent findings revealed the potential of proteins in hindering the corrosion phenomenon.[20] For instance, shrimp[21] and crab[22] waste proteins decreased the corrosion of low carbon steel in HCl and H_3PO_4 electrolytes, respectively.

Casein is the primary source of protein found in bovine milk.[23] This protein has recently found widespread industrial applications including medicine, food, and so forth.[24] However, there is still no literature on whether casein is capable of reducing the corrosion of aluminum in hydrochloric acid.

Therefore, in this research, the potential of casein in tackling the deterioration of aluminum in HCl was probed. Some analytical methods such as weight loss measurement, Tafel polarization, electrochemical impedance spectroscopy (EIS), and X-ray photoelectron spectroscopy (XPS) were utilized to assess the efficiency of the tested protein in minimizing the corrosion of AA1060. Based on the molecular structure, the additive might adsorb on aluminum and increase its corrosion resistance.

2 | EXPERIMENTAL PROCEDURE

In this research, the aluminum rectangular coupons with the dimensions of 35 × 20 × 2 (in mm) were cut from a main AA1060 sheet. Beside aluminum, the AA1060 specimens were composed of Si (0.25 wt%), Mn (0.03 wt%), Cu (0.05 wt%), and Fe (0.35 wt%).

To remove any surface contaminations, the specimens were abraded with SiC sandpapers up to #1800, immersed for a few seconds in acetone, rinsed with MilliQ water, and then quickly dried.

The additive-free corrosive electrolyte with a concentration of 0.1 M was prepared by diluting a suitable amount of HCl (37%; extra pure; ACS; VWR) with MilliQ water. In addition, to evaluate the ability of casein (Amicase; Sigma-Aldrich) in preventing the corrosion of AA1060, 50–500 ppm of this protein was added to the blank HCl solutions.

The changes in the weight of the aluminum coupons (called the weight loss analysis) were evaluated using an analytical balance (0.1 mg precision). The weight of the samples was compared before and after immersion in 250 mL of the prepared 0.1 M HCl solutions in the absence and presence of 50–500 ppm casein at different temperatures (between 298 K and 343 K). After 24 h, the coupons were taken out from the aggressive solutions, washed with a laboratory brush under running distilled water, rinsed with acetone, and dried with the airstream. Each experiment was carried out three times and the obtained data were employed to obtain the kinetic and thermodynamic data related to the corrosion of AA1060.

An electrochemical workstation (AUTOLAB potentiostat–galvanostat; PGSTAT30) was also utilized to investigate the changes in the corrosion resistance of the aluminum specimens immersed in the aggressive electrolyte without and with the inhibitor at room temperature. In this regard, a rectangular platinum sheet as a counter electrode, a saturated calomel electrode (SCE) as a reference electrode, and an AA1060 coupon as a working electrode were immersed in a corrosion test cell (PALM-IS-CCS; BASi) already filled with the corrosive electrolyte without and with 50–500 ppm casein. It should be noted that before inserting into the aggressive solution, the aluminum coupons were placed in a Teflon sample holder so that just 1 cm^2 of them was exposed.

After dipping an AA1060 working electrode in the solution, at first, its surface potential was monitored in the open circuit condition. The open circuit potential (OCP) as a function of time experiments was allowed to run until the corresponding plots reached a steady-state value. Then, the EIS analyses were conducted in the frequency range of 100 KHz–10 mHz. The EIS data were obtained at OCP by applying a small 10 mV alternating current signal to the cell. The Zview2 software was also employed to produce an equivalent electrical circuit and extract the electrochemical data from the Bode and Nyquist graphs. After EIS evaluations, the potentiodynamic polarization experiments were performed in the potential range between −300 and 300 mV versus OCP (with the potential scan rate of 5 mV/s). The obtained plots were analyzed using the Tafel extrapolation method, which yielded the corrosion potential (E_{corr}), together with the corrosion current density (i_{corr}) and the anodic (β_a), cathodic (β_c) slopes.

The surface of the aluminum coupons dipped in the blank and 500 ppm inhibitor-containing corrosive solutions

was evaluated by XPS (Thermo Escalab 250; detection limit: parts per thousand; base pressure: ca. 6×10^{-7} Pa). The survey spectra were acquired with an aluminum K_α X-ray source. The C (1s) peak observed at 284.8 eV was selected as the reference peak.

To probe the effects of casein on the surface topography and roughness of the AA1060 samples, a 10 μm × 10 μm area of the AA1060 coupons before and after immersion in the blank or the 500 ppm casein-amended electrolyte was characterized using the atomic force microscopy (AFM; Nanosurf Flex).

3 | RESULTS AND DISCUSSION

3.1 | Weight loss studies

Weight loss analysis is an efficient method used to elucidate the changes in the corrosion rate of a metallic substance exposed to an aggressive electrolyte in the absence or presence of an inhibitor.[25] Assuming that the AA1060 samples immersed in the blank or the casein-amended HCl solutions were uniformly corroded, the corrosion rate (CR; in $g\,m^{-2}\,h^{-1}$) of the specimens was calculated using Equation (1):

$$\text{Corrosion rate (CR)} = (\Delta W)/(A \times t), \tag{1}$$

where ΔW represents the decrease in the weight of the aluminum coupons (in grams; g) with the total surface area (in m^2; A) that occurred over a particular time interval (in hours; t).[26]

Moreover, the corrosion rate calculated before (CR_0) and after dissolving the different amounts of casein (CR) was utilized to determine the degree of the surface coverage (θ) of the tested protein (Equation 2). The efficiency of casein in tackling the corrosion phenomenon (i.e., corrosion inhibition efficiency; IE%) was also determined using Equation (3).[27]

$$\theta = \frac{CR_0 - CR}{CR_0}, \tag{2}$$

$$IE\% = \theta \times 100. \tag{3}$$

As indicated in Table 1 and Figure 1a,b, the concentration of casein in the aggressive electrolyte directly affects the corrosion rate of the AA1060 coupons, the surface coverage of the specimens, and the efficiency of casein in minimizing the calculated ΔW. For instance, when the content of the dissolved protein increased from 50 to 500 ppm at room temperature the IE% and θ values increased from 47.4% to 87.9% and from 0.47 to 0.87, respectively. In contrast, the rate at which the AA1060 specimens were corroded desirably dropped from $4.81\,g\,m^{-2}\,h^{-1}$ measured for the protein-free system to $0.58\,g\,m^{-2}\,h^{-1}$ obtained in the presence of 500 ppm casein. The observed changes could be ascribed to the geometric blocking effect of the casein molecules (i.e., the surface adsorption of the additive molecules on the active corroding regions of the metallic substrate).[28] This illustrates that the tested protein can be considered as an aluminum corrosion inhibitor in HCl.

However, changing the temperature of 0.1 M HCl solutions from 298 K to 343 K dramatically increased the corrosion rates of the metallic specimens dipped in the additive-free or the additive-containing solutions (e.g., from $0.58\,g\,m^{-2}\,h^{-1}$ without to $2.45\,g\,m^{-2}\,h^{-1}$ with 500 ppm protein) (Table 1). That means, increasing the solution temperature was accompanied by a decrease in the capability of the tested protein in reducing the corrosion of AA1060. This was probably because of the disintegration, configuration rearrangement, and/or detachment of the adsorbed casein molecules.[29] Similarly, the negative effects of increasing the electrolyte temperature on the efficiency of an aluminum corrosion inhibitor have been reported elsewhere.[30]

Moreover, it has been reported that an inhibitor affects the corrosion rate of aluminum by modifying the thermodynamic parameters of the corrosion process. This can be investigated using the Arrhenius equation (Equation 4) and the transition state theory (Equation 5).[31] In this regard, the corrosion rate values mentioned in Table 1 were utilized to evaluate the changes in the E_{act} (corrosion activation energy), the ΔS_{act} (entropy of activation), and the ΔH_{act} (enthalpy of activation) values[32]:

$$CR = A \exp\left(-\frac{E_{act}}{RT}\right), \tag{4}$$

$$CR = \frac{RT}{Nh} \exp\left(\frac{\Delta S_{act}}{R}\right) \exp\left(-\frac{\Delta H_{act}}{RT}\right), \tag{5}$$

where A, R, N, and h are the frequency factor, the universal gas constant, the experimental temperature in Kelvin, Avogadro's constant, and Plank's constant, respectively.

According to Equation (4), the corrosion activation energy was determined considering the plots in Figure 2a. While, based on Equation (5), the enthalpy of activation and entropy of activation values were obtained from the slope and the intercepts of the plots in Figure 2b, respectively.

As mentioned in Table 2, the E_{act} determined for the corrosion of the aluminum specimens in 0.1 M HCl solution was 6.52 kJ/mol, which increased to 27.54 kJ/mol when 500 ppm casein was added to the corrosive

TABLE 1 Data gathered from the weight loss experiments of the AA1060 coupons.

Solution temperature (K)	Inhibitor concentration (ppm)	Corrosion rate ($g\,m^{-2}\,h^{-1}$)	Surface coverage (θ)	Inhibitor efficiency (%)
298	0	4.81	–	–
	50	2.53	0.474	47.4
	100	1.62	0.663	66.3
	300	0.9	0.813	81.3
	500	0.58	0.879	87.9
313	0	5.35	–	–
	50	3.09	0.422	42.2
	100	2.11	0.605	60.5
	300	1.45	0.728	72.8
	500	1.01	0.811	81.1
328	0	6.03	–	–
	50	3.79	0.371	37.1
	100	2.78	0.538	53.8
	300	2.02	0.665	66.5
	500	1.71	0.716	71.6
343	0	6.79	–	–
	50	4.72	0.304	30.4
	100	3.75	0.447	44.7
	300	2.98	0.561	56.1
	500	2.45	0.639	63.9

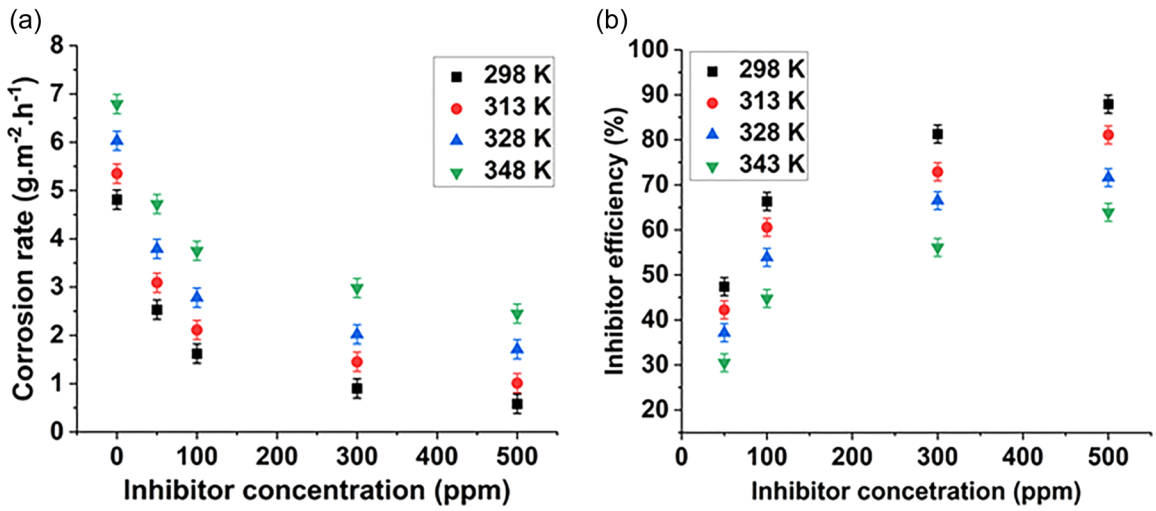

FIGURE 1 Changes in the "IE%" and the "CR" of AA1060 dipped in the 0.1 M HCl electrolyte without and with casein at temperature between 298 K and 343 K for 24 h. [Color figure can be viewed at wileyonlinelibrary.com]

electrolyte. The observed increase in the corrosion activation energy probably resulted from the adsorption of the tested protein on the surface of the metallic coupons, which increased the thickness of the formed double layer.[33]

Moreover, the presence of the inhibitor molecules in the electrolyte increased ΔH_{act} (e.g., from 3.9 to 24.9 kJ/mol) confirming the positive role of the tested additive in inhibiting the corrosion of the AA1060 coupons.

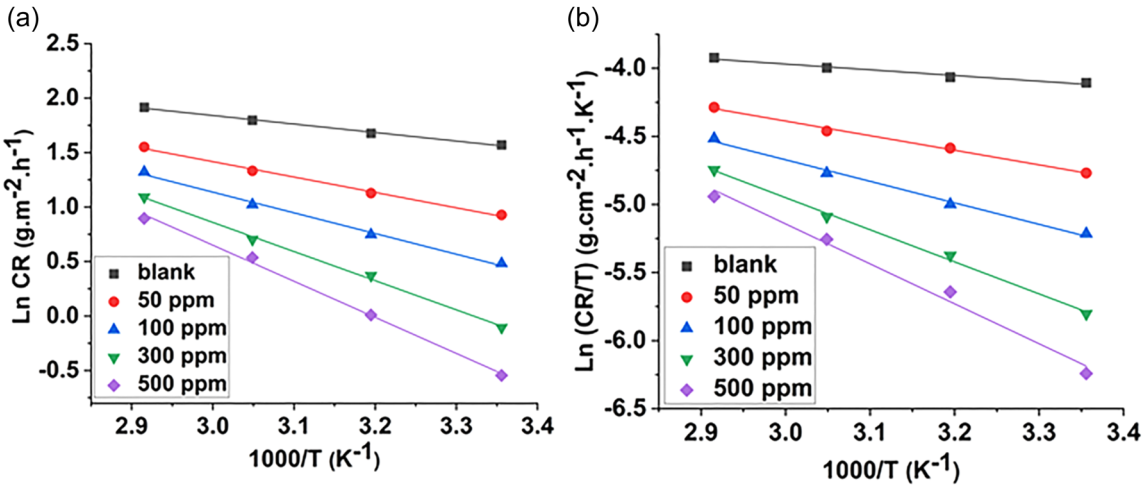

FIGURE 2 (a) Arrhenius and (b) transition state theory plots obtained from the weight loss data of the AA1060 samples. [Color figure can be viewed at wileyonlinelibrary.com]

TABLE 2 Thermodynamic parameters calculated for the corrosion of AA1060 samples immersed in the blank or the casein-amended HCl solutions.

Concentration	E_{act} (kJ/mol)	ΔH_{act} (kJ/mol)	ΔS_{act} (J mol^{-1} K^{-1})
Blank	6.52	3.9	−218.9
50 ppm	11.73	9.1	−206.84
100 ppm	15.79	13.1	−196.9
300 ppm	21.99	19.6	−179.9
500 ppm	27.54	24.9	−165.8

In addition, the positive sign of the enthalpy of activation illustrates the endothermic nature of the aluminum corrosion process.[34]

Furthermore, as indicated in Table 2, the ΔS_{act} value in the absence of the additive was −218.9 J mol^{-1} K^{-1}, while it became less negative (i.e., −165.8 J mol^{-1} K^{-1}) with 500 ppm casein. This variation in ΔS_{act} further confirms the adsorption of the inhibitor molecules on the surface of aluminum, which replaced the water molecules already present in the vicinity of the specimens. It also illustrates that during the adsorption phenomenon, the degree of disorder in the system decreases.[35] This is in agreement with another report where the corrosion of aluminum was inhibited with an organic compound.[16]

3.2 | Adsorption studies

To further elucidate how casein reduced the corrosion rate of the AA1060 specimens, the weight loss data (Table 1) were fitted to the common adsorption isotherms (i.e., Langmuir, Freundlich, Temkin, and Flory–Huggins isotherms) with the following equations (Figure 3)[36]:

$$\text{Langmuir: } \frac{C}{\theta} = \frac{1}{k_{ads}} + C. \quad (6)$$

$$\text{Freundlich: } \theta = k_{ads} C^{1/n}. \quad (7)$$

$$\text{Temkin: } \exp(f\theta) = k_{ads} C. \quad (8)$$

$$\text{Flory} - \text{Huggins}: \frac{\theta}{[e^{(1-x)} \times (1-\theta)^x]} = k_{ads} C, \quad (9)$$

where C is the concentration of the inhibitor in the solution, θ is the surface coverage, k_{ads} is the adsorption–desorption equilibrium constant, f is the energetic inhomogeneity factor, and n is the heterogeneity parameter ($0 < n < 1$).

Considering the R^2 values, the adsorption of casein on the AA1060 samples at 298 K was based on the Langmuir adsorption isotherm ($R^2 = 0.999$) rather than the Freundlich, Temkin, and Flory–Huggins isotherms for which the R^2 values of 0.936, 0.970, and 0,987 were calculated, respectively.

In addition, the Langmuir isotherm equation was employed to evaluate the adsorption of casein on the AA1060 samples at the other tested temperatures (Figure 4). It was observed that the R^2 values determined at the other tested temperatures were between 0.99 and 1, illustrating that the adsorbed inhibitor molecules did not interact with each other. Moreover, based on the Langmuir adsorption theory,

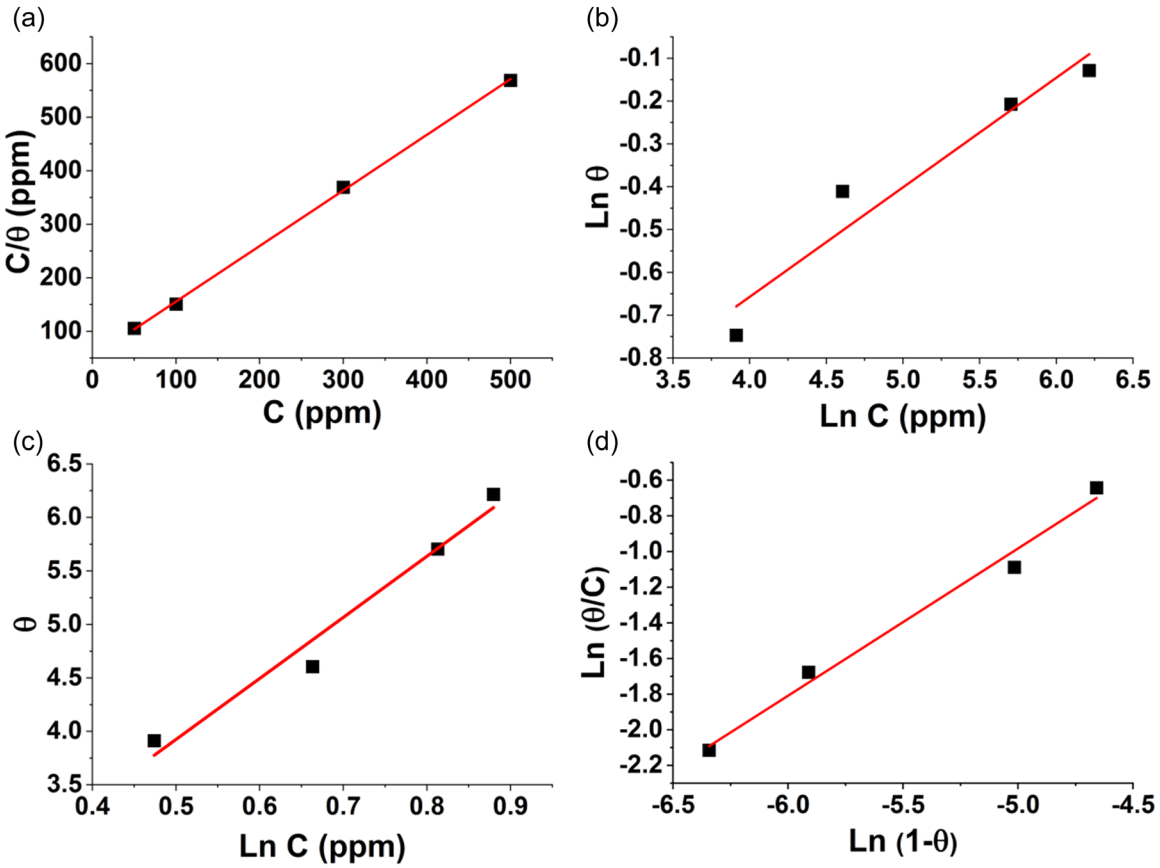

FIGURE 3 Graphs of (a) Langmuir; (b) Freundlich; (c) Temkin; and (d) Flory–Huggins isotherms calculated for the adsorption of casein on the surface of the AA1060 specimens in 0.1 M HCl at 298 K. [Color figure can be viewed at wileyonlinelibrary.com]

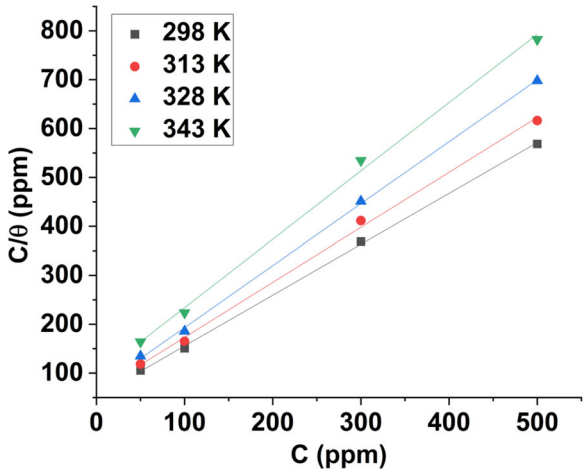

FIGURE 4 Langmuir isotherm plots related to the adsorption of the tested protein on the AA1060 specimens in HCl at different temperatures. [Color figure can be viewed at wileyonlinelibrary.com]

the additive molecules formed a monolayer on the surface of the specimens.[37]

The adsorption of casein on aluminum was further investigated by calculating the free energy of adsorption (ΔG^{o}_{ads}) (Equation 10) (Table 3)[38]:

TABLE 3 Casein adsorption data determined for the inhibition of the AA1060 coupons in 0.1 M HCl at different temperatures.

Temperature (K)	K_{ads} (mg/L)	ΔG^{o}_{ads} (kJ/mol)
298	0.0193	−24.46
313	0.0164	−24.06
328	0.0150	−23.83
343	0.0106	−22.97

$$\Delta G^{o}_{ads} = -RT \ln (K_{ads} \times C_{solvent}). \quad (10)$$

In this regard, K_{ads} (i.e., the equilibrium constant of the adsorption process) was obtained by inverting the intercept of the lines plotted in Figure 4. $C_{solvent}$ was also considered as 10^6 mg/L for a water-based solvent.

The results mentioned in Table 3 indicate that increasing the temperature of 0.1 M HCl from 298 K to 343 K adversely decreased the K_{ads} values from 0.0193 to 0.0106 mg/L. Meanwhile, ΔG^{o}_{ads} increased, for example, from −24.46 kJ/mol at 298 K to −22.97 kJ/mol at 343 K, revealing the exothermic nature of the casein adsorption on AA1060. That means increasing the temperature

results in the desorption of the inhibitor molecules and unfavored the corrosion inhibition process.[39] It has also been demonstrated that an exothermic adsorption phenomenon indicates the occurrence of both types of adsorption (i.e., physical and chemical), while an endothermic interaction is just related to chemisorption.

Furthermore, the negative sign of ΔG°_{ads} illustrates that the corrosion inhibitor (e.g., casein) spontaneously adsorbed on the substrate (e.g., AA1060) and the adsorbed molecules were stable on the tested coupons.[40] Moreover, it has been highlighted that a ΔG°_{ads} value between zero and −20 kJ/mol indicates the electrostatic interactions between the inhibitor molecules and the metallic adsorbent (physisorption), whilse a corresponding value more negative than −40 kJ/mol reveals the charge sharing between the organic adsorbate and the metal surface (chemisorption). In contrast, ΔG°_{ads} between −20 and −40 kJ/mol represents both physisorption and chemisorption phenomena.[41] Therefore, considering the ΔG°_{ads} values mentioned in Table 3, which were between −24.46 and – 22.97 kJ/mol, it can be said that both physisorption and chemisorption happened during the adsorption of casein on the AA1060 specimens.

3.3 | Electrochemical measurements

The aluminum corrosion inhibition potential of casein was further evaluated using some electrochemical techniques. At first, the OCP of the samples in the absence and presence of 50–500 ppm casein was evaluated at 298 K (Figure 5). This analysis reveals any changes in the zero-current potential created between

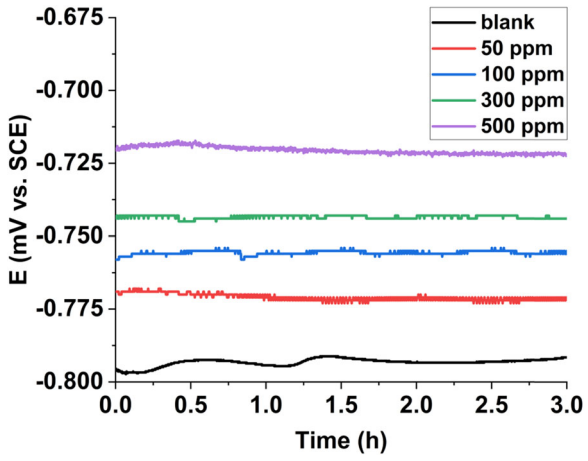

FIGURE 5 Open circuit potential graphs related to the electrochemical analyses of the AA1060 samples dipped in the blank or the casein-amended 0.1 M HCl at 298 K. [Color figure can be viewed at wileyonlinelibrary.com]

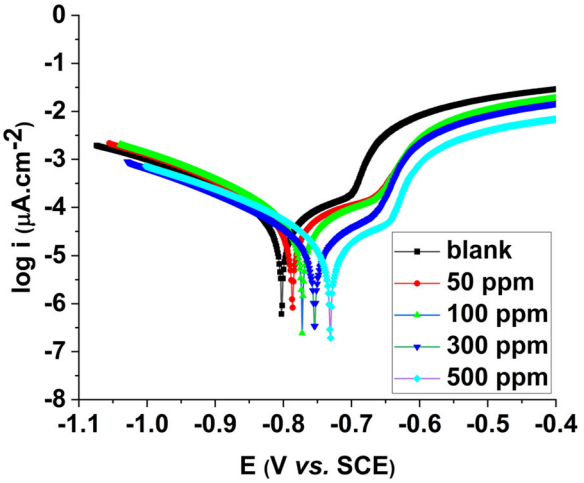

FIGURE 6 The polarization curves related to the electrochemical analyses of the AA1060 specimens immersed in 0.1 M HCl in the absence and presence of different amount of casein at 298 K. [Color figure can be viewed at wileyonlinelibrary.com]

the aluminum working electrodes and the corrosive electrolyte with respect to the SCE. It is evident that in the blank solution, after some fluctuations the OCP plot stayed almost constant at about −791 mV after 3 h.

In comparison, when casein was dissolved in the corrosive electrolyte, the OCP plots were almost stable from the beginning. Moreover, 50, 100, 300, or 500 ppm casein increased the OCP values measured after 3 h to −771, −755, −742, −720 mV, respectively. This could be due to the surface adsorption of the tested additive which made a barrier between the working electrodes and the corrosive solution. Here, it is worth mentioning that although in this research the presence of the tested inhibitor made the OCP values more positive, in other literature, a negative shift in OCP was observed for example when some Schiff bases were used as corrosion inhibitors to prevent the corrosion of AA1060 in HCl.[42]

The role of casein in reducing the deterioration of aluminum in 0.1 M HCl was also assessed using the potentiodynamic polarization technique at room temperature (Figure 6). It can be seen that the plots were composed of a cathodic and an anodic region where the reactions related hydrogen evolution and the aluminum dissolution took place, respectively.[43]

The Tafel extrapolation method was utilized to determine the potential at which the cathodic and anodic reaction equalize (i.e., corrosion potential; E_{corr}), the current produced during the corrosion phenomena per unit area (i.e., corrosion current density; i_{corr}) and the Tafel slopes (β_a, β_c) which reveal the relationship between the electrode potential and the current produced in an electrochemical cell (Table 4). In addition, the calculated corrosion current densities and the Tafel

TABLE 4 The Tafel extrapolation data related to the corrosion of AA1060 specimens in 0.1 M HCl in the absence and presence of the tested protein at 298 K.

Concentration	E_{corr} (mV vs. SCE)	I_{corr} (μA/cm^2)	β_a (mV/dec)	$-\beta_c$ (mV/dec)	R_{pol} (Ω cm^2)
Blank	−802.7	63.09	192.6	170.8	62.3
50 ppm	−786.1	34.7	173.6	123.7	90.3
100 ppm	−772.3	23.3	162.8	106.5	119.9
300 ppm	−754.6	11.9	146.7	100.1	217.1
500 ppm	−730.5	6.1	138.5	98.7	410.2

slopes were employed to determine the variations in the polarization resistance of the AA1060 coupons (R_p) in the absence and presence of casein (Equation 11)[44]

$$R_P = \frac{(\beta_a \times \beta_c)}{2.303 \times i_{corr} \times (\beta_a + \beta_c)}. \quad (11)$$

According to Table 4, the i_{corr} value for the protein-free system was 63.09 μA/cm^2. However, increasing the concentration of protein from 50 to 500 ppm considerably decreased the i_{corr} from 37.4 to 6.1 μA/cm^2. In contrast, the corrosion potential shifted towards the positive values so that the presence of 500 ppm casein yielded E_{corr} of −730.6 mV compared to −802.7 mV obtained for the blank solution.

It is worth noting that E_{corr} can be used to classify a corrosion inhibitor as a cathodic, an anodic or a mixed type.[45] It has been suggested that if the absolute value of the difference between the corrosion potential measured in the presence of a corrosion inhibitor and the corresponding value obtained from the control solution is more than 85 mV, the additive is a cathodic or an anodic type. Otherwise, the tested inhibitor is a mixed type. With 500 ppm casein, a 73 mV shift in E_{corr} towards the positive values was observed indicating the mixed-type property of the tested inhibitor where the anodic behavior was almost dominant (i.e., the additive preferentially adsorbed on the anodic regions of the AA1060 specimens). Moreover, the tested protein altered both cathodic and anodic Tafel slopes, further demonstrating its mixed-type behavior. In another research, guar gum was similarly considered as a mixed-type corrosion inhibitor where it was used to inhibit the corrosion of aluminum in 1 M HCl.[26]

The changes in the polarization resistance (R_p) of the metallic coupons also reveal the effectiveness of an inhibitor. It is noticeable that in the absence of casein, R_p was about 0.632 kΩ cm^2 which increased to 4.102 kΩ cm^2 when 500 ppm casein was present in the electrolyte. The measured increase indicates that casein adsorbed on the surface of the AA1060 coupons which made a barrier between the working electrode and the solution. In other words, the dissolved protein modified the mass and the charge transfer reactions at the metal/solution interfaces.[46]

EIS was also employed to illustrate the ability of casein in inhibiting the corrosion of aluminum in hydrochloric acid. The produced data were presented as Nyquist and Bode phase angle graphs.

It is evident from Figure 7 that the EIS Nyquist plots were in elliptic shape composed of a single semicircle called a "capacitive loop" and an "inductive" loop that occurred at the high and low frequencies, respectively. This shape is also observed by other researchers where the corrosion of aluminum in HCl was investigated.[47,48]

The occurrence of a capacitive loop at high frequencies can probably be attributed to the charge transfer during the corrosion process, mass transfer, and/or frequency dispersion phenomena.[49] In addition, it has been proposed that the capacitive loop might be observed because of the presence of a surface oxide layer on the working electrodes which acts as a double layer.[17] This loop can also be observed due to the interfacial reactions occurred at the aluminum/aluminum oxide/solution interface. As an example, after dipping an aluminum working electrode in the corrosive electrolyte, at first Al^+ is formed at the aluminum/aluminum oxide interface, then the formed cations migrate through the aluminum oxide layer to the aluminum oxide/solution interface where they are oxidized to Al^{3+}.[50] Moreover, the occurrence of a capacitive loop can be related to the presence of an inhibitor in the solution which resulted in the formation of some complexes such as $[metal\text{-}oxide\text{-}hydroxide\text{-}inhibitor]_{ads}$.

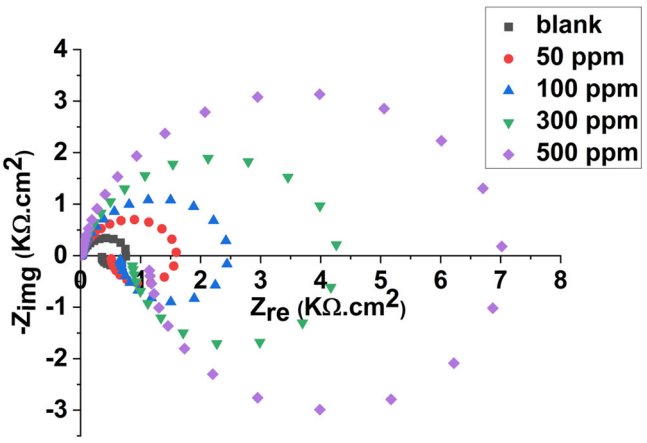

FIGURE 7 Nyquist graphs related to the electrochemical analyses of AA1060 coupons immersed in 0.1 M HCl in the absence and presence of the different amount of casein after 3 h at 298 K. [Color figure can be viewed at wileyonlinelibrary.com]

On the other hand, the formation of the inductive loop is still under debate and might be originated from the adsorption of the charged species such as H^{+}_{ads}, Cl^{-}_{ads}, and/or the inhibitor species.[51] Focusing on the Nyquist plots, reveals the bigger diameter of the ellipses recorded in the presence of casein compared to that obtained from the blank solution denoting the effectiveness of casein in increasing the impedance of working electrodes. The changes in the EIS plots were further quantified using an electrical equivalent circuit (Figure 8). The proposed circuit was composed of some elements. The R_s was used to evaluate the changes in the solution resistance between the SCE electrode and the working electrode. R_{ct} denotes any resistance to the charge transfer at the working electrode/electrolyte interface and indicates the diameter of the capacitive semicircle. This parameter is also inversely proportional to the rate at which a working electrode is getting corroded.[52]

Once a working electrode is immersed in the corrosive electrolyte, a double layer is formed at the vicinity of the electrode. The capacity of the formed structure in an ideal condition is shown by C_{dl}. However, in reality, due to the surface roughness and inhomogeneity, the presence of impurities such as grain boundaries, and the adsorption of some species, a constant phase element (CPE) is used instead of C_{dl} representing the deviations from an ideal behavior.[16] The impedance of CPE (Z_{CPE}) is obtained using Equation (12).[53]

$$Z_{CPE} = Y^{-1}(j\omega)^{-n}. \quad (12)$$

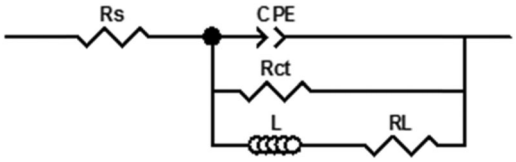

FIGURE 8 The equivalent circuit employed to fit the electrochemical impedance spectroscopy graphs.

Equation (12) includes ω (rad/s) as an angular frequency, Y ($\Omega^{-1}\,S^{n}\,cm^{-2}$) which is the magnitude of CPE, and $j = (-1)^{1/2}$. In addition, CPE is composed of CPE-T and n as the characteristic parameters where n is an empirical exponent ($0 \le n \le 1$) which indicates any deviation from the ideal capacitive condition.[26] Besides, an inductance (L; $H\,cm^2$) together with an inductive resistance (R_L; $\Omega\,cm^2$) were considered in the suggested circuit.

The results from the fitting procedure revealed an increase in R_{ct} from 1753 to 7458 $\Omega\,cm^2$ when the amount of casein dissolved in the system increased from 50 to 500 ppm. Whilst, the corresponding value for the uninhibited sample was 907.4 $\Omega\,cm^2$ (Table 5).

In addition, a higher CPE-T value of ~$3.1 \times 10^{-4}\,\Omega^{-1}\,S^{n}\,cm^{-2}$ was obtained for the sample immersed in the protein-free solution compared to those dipped in the casein containing electrolytes (e.g., $1.17 \times 10^{-5}\,\Omega^{-1}\,S^{n}\,cm^{-2}$ with 500 ppm casein). This is attributed to the adsorption of the tested protein on the working electrodes which resulted in an increase in the thickness of the electrical double layer.[54] Moreover, the decrease in the CPE values with the inhibitor can be because of the replacement of the adsorbed water molecules by the corrosion inhibitor molecules with a lower dielectric constant.

Furthermore, in the presence of the tested corrosion inhibitor, the fitted values for n slightly increased, for example, from 0.85 obtained for the inhibitor-free experiment to 0.9 with 500 ppm casein. The observed increase could be due to the adsorption of the inhibitor molecules on the AA1060 samples which increased the surface homogeneity.

Similar to the R_{ct} values, changing the concentration of protein in the solution from 50 to 500 ppm, increased the L and R_L values from 1951 to 6252 $H\,cm^2$ and from 692 to 1298 $\Omega\,cm^2$, respectively. Whilst, in the blank 0.1 M HCl solution the $L = 1255\,H\,cm^2$ and $R_L = 556\,\Omega\,cm^2$ were obtained. This is compatible with the previous

TABLE 5 EIS data related to the corrosion of AA1060 dipped in 0.1 M HCl in the absence and presence of casein at 298 K.

	R_s ($\Omega\,cm^2$)	CPE-T ($\Omega^{-1}\,S^{n}\,cm^{-2}$)	n	R_{ct} ($\Omega\,cm^2$)	L ($H\,cm^2$)	R_L ($\Omega\,cm^2$)
Blank—3 h	8.9	3.1×10^{-4}	0.85	907.4	1255	556
Blank—24 h	8.7	5.21×10^{-4}	0.84	621.3	1047	481
50 ppm—3 h	11.26	7.59×10^{-5}	0.87	1753	1951	692
100 ppm—3 h	11.72	4.64×10^{-5}	0.88	2701	2291	851
300 ppm—3 h	11.56	3.16×10^{-5}	0.88	4673	4721	1028
500 ppm—3 h	10.272	1.17×10^{-5}	0.9	7458	6327	1321
500 ppm—24 h	10.1	2.52×10^{-5}	0.89	7356	6252	1298

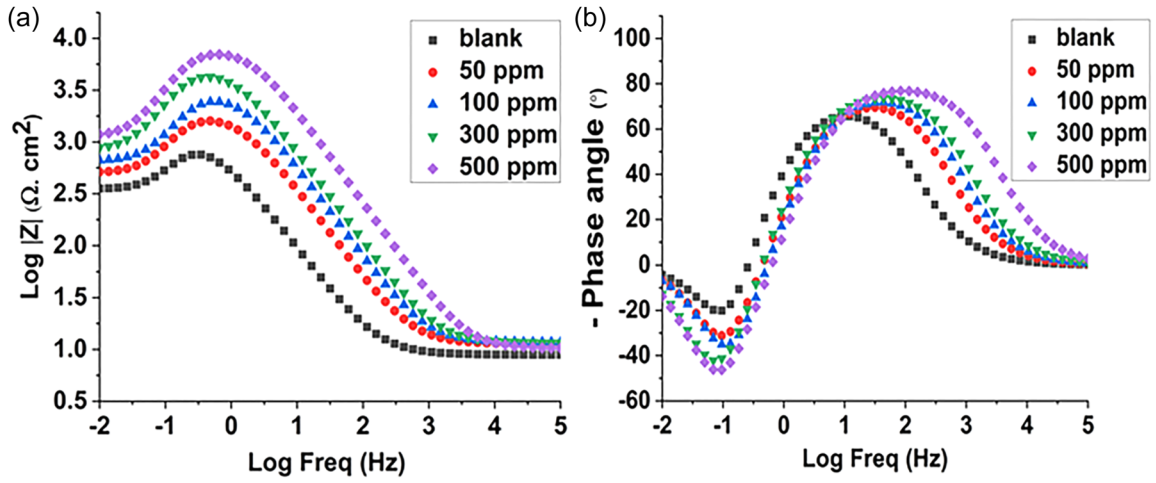

FIGURE 9 (a) Bode and (b) phase angle graphs obtained from the electrochemical analyses of the AA1060 samples dipped in 0.1 M HCl in the absence and presence of casein at 298 K. [Color figure can be viewed at wileyonlinelibrary.com]

studies in which further dissolving of a corrosion inhibitor was accompanied by an increase in L and R_L.[55]

The EIS data were also presented as Bode plots (Figure 9a,b). Based on the corresponding plots, the efficiency of a corrosion inhibitor is evaluated using the impedance modulus ($|Z|$). Therefore, comparing the log $|Z|$ values at log $f = -2$, it is apparent that the highest impedance modulus appeared when 500 ppm casein was added to the corrosive electrolyte (Figure 9a). In addition, the appearance of one peak at high frequencies (log f between 1 and 2) and one valley at low frequencies (about log $f = -1$) further demonstrate the presence of a capacitive and an inductive loop in the Nyquist graphs, respectively (Figure 9b). It can also be seen that the phase angle values recorded in the presence of casein were higher than those obtained for the blank system revealing the adsorption of the inhibitor molecules and formation of a protective layer on the surface of the AA1060 specimens. Furthermore, the phase angle plots displayed a continuous shift when the concentration of the inhibitor increased from 50 to 500 ppm demonstrating the direct relationship between the effectiveness of casein and its concentration.

The efficiency of the adsorbed casein molecules in inhibiting the corrosion of AA1060 samples were further evaluated by repeating the EIS experiment for the working electrodes dipped in the blank and 500 ppm protein-containing electrolytes for 24 h. The obtained data were compared with those collected after 3 h (Figure 10). After 24 h, a dramatic decrease in the R_{ct} value (from 907.4 to 621.3 $\Omega\,cm^2$) was recorded for the uninhibited specimen. Whereas, with 500 ppm casein, a negligible drop in R_{ct} (from 7458 to 7356 $\Omega\,cm^2$) was measured confirming the stability of the adsorbed protein molecules on the surface of AA1060.

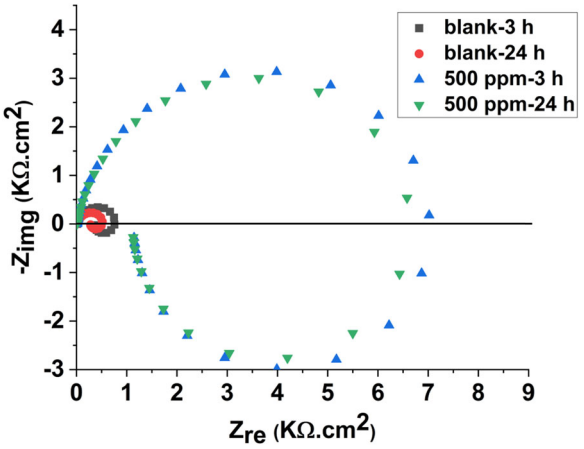

FIGURE 10 Nyquist plots related to the corrosion of AA1060 sample immersed in the blank and 500 ppm casein-amended electrolytes for 3 and 24 h at 298 K. [Color figure can be viewed at wileyonlinelibrary.com]

3.4 | XPS analysis

The adsorption of casein on the surface of the AA1060 specimens was further demonstrated by XPS spectroscopy. In this regard, the surface of an AA1060 coupon placed in the 500 ppm casein-containing solution for 24 h at 298 K was characterized (Figure 11). According to the XPS full-survey spectra, the Al 2p and O 1s peaks detected at the binding energies of 74.55 and 531.51 eV, respectively, are related to Al_2O_3 formed on the surface of the specimen after taking it out from the solution. Moreover, the detection of N 1s signal at the binding energy of 399.37 eV originates from the casein molecules adsorbed on the surface of the specimen and prevented it from corrosion. This is in accordance

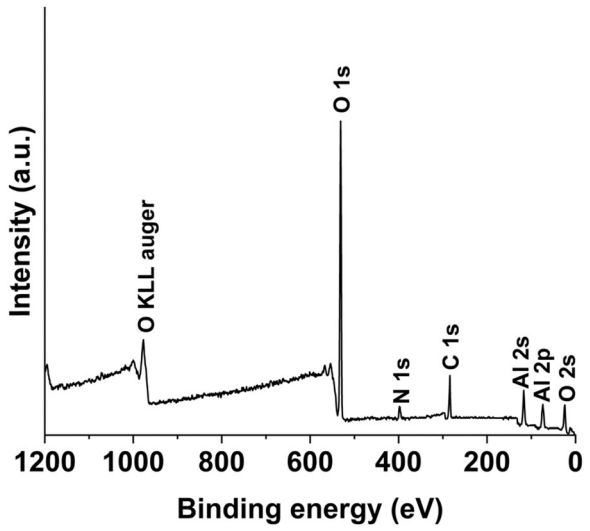

FIGURE 11 X-ray photoelectron spectroscopy full-survey spectra related to a AA1060 sample immersed in the 500 ppm casein-amended 0.1 M HCl for 24 h at 298 K.

with the data reported by the others where the detection of N in the XPS spectra was related to the adsorption of a corrosion inhibitor containing nitrogen in its molecular structure.[56]

3.5 | AFM analysis

The role of the tested protein in reducing the corrosion of AA1060 specimens was further assessed by comparing the surface topography of the as-polished coupon with those immersed in the blank and the 500 ppm casein-amended corrosive electrolyte for 24 h at 298 K (Figure 12).

It can be seen from the three-dimensional patterns that due to proper polishing with the emery papers just minor scratches were present on the surface of the as-polished sample and the *Ra* value was about 26 nm (Figure 12a). Whereas, the AA1060 specimen immersed in the casein-free HCl solution was severely corroded and had a very uneven surface with $Ra = 147.4$ nm (Figure 12b). In comparison, when 500 ppm protein was added to the corrosive media, the formation of a protective layer by the protein molecules caused a relatively smooth surface (with $Ra = 64$ nm) with negligible signs of corrosion (Figure 12c). To shed light on the effects of casein in reducing the surface roughness of the corroded AA1060 specimen, the height profile of the samples is also presented (Figure 12d). The decrease in the surface roughness of the aluminum specimens in the presence of a corrosion inhibitor has also been illustrated by others.[57,58]

3.6 | Mechanism of inhibition

Based on the literature, there are wide varieties of organic molecules and inorganic ions available to decrease the corrosion rate of the metallic specimens.[59] It has also been proposed that the inhibitor molecules diffuse, adsorb and interact with a surface so that they form a protective layer at the metal/solution interface.[50]

Considering the ΔG^{o}_{ads} values illustrated in this research, it is evident that casein interacted with the AA1060 specimens via both chemical and physical adsorptions. Hence, a combination of the following mechanisms may occur to inhibit the corrosion of the working electrodes in 0.1 M HCl.

(i) Electrostatic adsorption: In HCl, the oxygen and/or nitrogen atoms present in the molecular structure of casein interact with H^+, and get protonated. On the other hand, in the acidic solutions the oxide or the hydroxide layer already formed on the surface of aluminum is protonated and forms Al–OH_2^+ species. Thus, the surface of the aluminum working electrodes has a positive charge.[26] The aluminum coupons with positive surface charge, electrostatically attract the Cl^- ions already present in the solution. Therefore, the accumulation of the chloride ions at the metal/solution interface, favors the adsorption of the positively charged casein molecules.

In another mechanism, the following reactions have been suggested for the dissolution of aluminum in HCl[30]:

$$Al + Cl^- \leftrightarrow AlCl^-_{ads}, \quad (13)$$

$$AlCl^-_{ads} + Cl^- \rightarrow AlCl_2^+ + 3e^-. \quad (14)$$

The deprotonated casein molecules interact with $AlCl^-_{ads}$ species via electrostatic force and prevent the reaction (14) to occur.[30]

(ii) Chemisorption: This type of adsorption occurs as a result of the coordinated types of bonding onset between the nonbonding pairs of electrons present in a heteroatom such as oxygen and the vacant p-orbital of the aluminum atoms. The presence of oxygen atoms with a lone pair of electrons in the molecular structure of casein, allows this protein to combine with Al^{3+} and make metal-inhibitor complexes. Then, the formed $[inhibitor\text{-}Al]^{2+}$ complexes get adsorbed onto the working electrode by van der Waals force and make a barrier layer to prevent the corrosion of aluminum.[17]

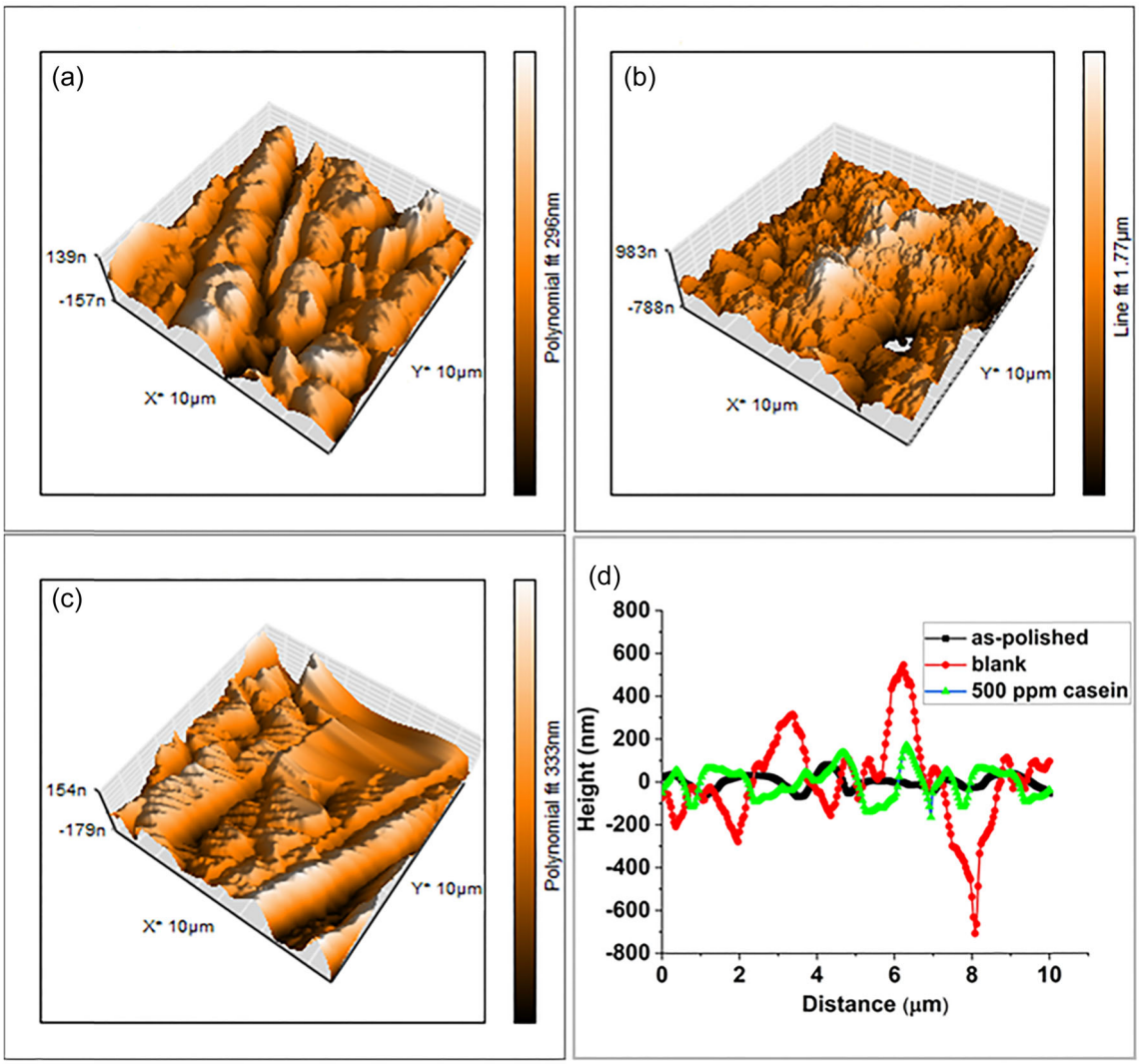

FIGURE 12 Atomic force microscopy analysis of the AA1060 coupons (a) before immersion; (b) immersed in 0.1 M HCl at room temperature for 24 h without, and (c) with 500 ppm casein; (d) variations in the height of the analyzed specimens. [Color figure can be viewed at wileyonlinelibrary.com]

4 | CONCLUSION

The effectiveness of casein as a biodegradable protein in inhibiting the corrosion of AA1060 in 0.1 M HCl was investigated. It was revealed that in the presence of casein, the weight loss and the corrosion rate of the aluminum coupons were considerably decreased. This was due to the adsorption of casein on the surface of the specimens and the formation of a protective layer at the metal/electrolyte interface. Whereas, increasing the temperature of the corrosive solution from 298 K to 343 K adversely reduced the corrosion inhibitory efficiency of casein.

Based on the thermodynamic and kinetic evaluations, both physisorption and chemisorption phenomena occurred during the adsorption of casein on the working electrodes resulting in an increase in the amount of energy required for the initiation of corrosion. In addition, it was illustrated that the adsorption of casein was best fitted with the Langmuir adsorption isotherm.

The electrochemical analyses further demonstrated the inhibitory potential of casein. For instance, increasing the amount of casein decreased the corrosion current density. Moreover, an increase in the charge transfer resistance and the double layer thickness was recorded when casein was already dissolved in the system. Further, the surface topography illustrated a remarkable decrease in the corrosion induced damages. The formation of a protective film that prevented the corrosive ions from interacting with the aluminum coupons was further disclosed.

ACKNOWLEDGMENTS

This work was supported by the University of Tabriz.

CONFLICT OF INTEREST STATEMENT

The authors declare no conflict of interest.

DATA AVAILABILITY STATEMENT

The data that support the findings of this study are available from the corresponding author upon reasonable request.

ORCID

Taher Rabizadeh http://orcid.org/0000-0003-3483-2764

REFERENCES

[1] S. R. S. Rodrigues, V. Dalmoro, J. H. Z. Santos, *Mater. Corros.* **2020**, *71*, 1160.
[2] T. Dursun, C. Soutis, *Mater. Des.* **2014**, *56*, 862.
[3] S. John, A. Joseph, *Mater. Corros.* **2013**, *64*, 625.
[4] D. G. Ladha, N. K. Shah, Z. Ghelichkhah, I. B. Obot, F. Khorrami Dehkharghani, J. Z. Yao, D. D. Macdonald, *Mater. Corros.* **2018**, *69*, 125.
[5] K. Malakhova, L. V. Zaitseva, R. G. Zinchenko, *Chem. Pet. Eng.* **1972**, *8*, 736.
[6] M. R. Ortega Vega, S. Mattedi, R. M. Schroeder, C. Fraga Malfatti, *Mater. Corros.* **2021**, *72*, 543.
[7] G. I. Ramírez-Peralta, U. León-Silva, M. E. Nicho Diaz, M. G. Valladares-Cisneros, *Mater. Corros.* **2018**, *69*, 1631.
[8] T. Rabizadeh, S. Khameneh Asl, *Mater. Corros.* **2019**, *70*, 738.
[9] Y. Xiao-Ci, Z. Hong, L. Ming-Dao, R. Hong-Xuan, Y. Lu-An, *Corros. Sci.* **2000**, *42*, 645.
[10] K. F. Khaled, M. M. Al-Qahtani, *Mater. Chem. Phys.* **2009**, *113*, 150.
[11] M. Abdallah, M. Sobhi, H. M. Altass, *J. Mol. Liq.* **2016**, *223*, 1143.
[12] T. L. Chen, H. Kim, S. Y. Pan, P. C. Tseng, Y. P. Lin, P. C. Chiang, *Sci. Total Environ.* **2020**, *716*, 136998.
[13] T. Guldberg Klenø, L. Rønnedal Leonardsen, H. Ørsted Kjeldal, S. Møller Laursen, O. Nørregaard Jensen, D. Baunsgaard, *Proteomics* **2004**, *4*, 868.
[14] Z. Q. Shi, Y. S. Liu, Q. Xiong, W. W. Cai, G. G. Ying, *Sci. Total Environ.* **2019**, *661*, 407.
[15] M. Djellab, H. Bentrah, A. Chala, H. Taoui, *Mater. Corros.* **2019**, *70*, 149.
[16] Y. T. Du, H. L. Wang, Y. R. Chen, H. P. Qi, W. F. Jiang, *J. Environ. Chem. Eng.* **2017**, *5*, 5891.
[17] X. Li, S. Deng, *Corros. Sci.* **2012**, *65*, 299.
[18] D. I. Njoku, I. Ukaga, O. B. Ikenna, E. E. Oguzie, K. L. Oguzie, N. Ibisi, *J. Mol. Liq.* **2016**, *219*, 417.
[19] A. Khadraoui, A. Khelifa, K. Hachama, R. Mehdaoui, *J. Mol. Liq.* **2016**, *214*, 293.
[20] T. Rabizadeh, S. K. Asl, *J. Mol. Liq.* **2019**, *276*, 694.
[21] A. A. Farag, A. S. Ismail, M. A. Migahed, *Egypt. J. Pet.* **2018**, *27*, 1187.
[22] A. S. Ismail, A. A. Farag, *Surf. Interfaces* **2020**, *19*, 100483.
[23] D. Jakubowicz, O. Froy, *J. Nutr. Biochem.* **2013**, *24*, 1.
[24] L. Liang, Y. Luo, *Trends Food Sci. Technol.* **2020**, *97*, 391.
[25] D. Wang, Y. Li, T. Chang, A. Luo, *Colloids Surf. A*, **2021**, *628*, 127308.
[26] X. Rao, L. Zhou, G. Zhang, X. Wang, S. Xia, L. Yu, *Mater. Corros.* **2020**, *71*, 1521.
[27] L. A. L. Guedes, K. G. Bacca, N. F. Lopes, E. M. da Costa, *Mater. Corros.* **2019**, *70*, 1288.
[28] E. E. Oguzie, *Corros. Sci.* **2007**, *49*, 1527.
[29] R. S. Nathiya, S. Perumal, V. Murugesan, V. Raj, *Mater. Sci. Semicond. Process.* **2019**, *104*, 104674.
[30] S. Deng, X. Li, *Corros. Sci.* **2012**, *64*, 253.
[31] V. K. K., A. R. BV, *New J. Chem.* **2017**, *41*, 6278.
[32] C. Gao, X. Zhao, K. Liu, X. Dong, S. Wang, F. Kong, *Mater. Corros.* **2020**, *71*, 1903.
[33] I. B. Obot, N. O. Obi-Egbedi, S. A. Umoren, *Int. J. Electrochem. Sci.* **2009**, *4*, 863.
[34] D. Kumari, P. P. Venugopal, P. D. Reena Kumari, D. Chakraborty, *J. Adhes. Sci. Technol.* **2022**, *36*, 2020.
[35] M. Abdallah, *Corros. Sci.* **2004**, *46*, 1981.
[36] I. B. Obot, N. O. Obi-Egbedi, *Colloids Surf. A*, **2008**, *330*, 207.
[37] I. B. Onyeachu, D. S. Chauhan, K. R. Ansari, I. B. Obot, M. A. Quraishi, A. H. Alamri, *New J. Chem.* **2019**, *43*, 7282.
[38] E. Berdimurodov, A. Kholikov, K. Akbarov, L. Guo, S. Kaya, K. P. Katin, D. K. Verma, M. Rbaa, O. Dagdag, *Colloids Surf. A*, **2022**, *633*, 127837.
[39] A. S. Fouda, M. A. Ismail, A. M. Temraz, A. S. Abousalem, *New J. Chem.* **2019**, *43*, 768.
[40] Q. Zhang, Z. Gao, F. Xu, X. Zou, *Colloids Surf. A*, **2011**, *380*, 191.
[41] H. Li, Y. Qiang, W. Zhao, S. Zhang, *Colloids Surf. A*, **2021**, *616*, 126077.
[42] U. Nazir, Z. Akhter, N. Z. Ali, F. U. Shah, *RSC Adv.* **2019**, *9*, 36455.
[43] Q. Yuan, R. Cheng, S. Zou, C. Ding, H. Liu, Y. Wang, D. Yang, X. Xiao, Q. Jiang, R. Tang, J. Chen, *J. Mater. Res. Technol.* **2020**, *9*, 11935.
[44] M. R. El Sayed Aly, H. Shokry, T. Sharshar, M. A. Amin, *J. Mol. Liq.* **2016**, *214*, 319.
[45] D. Prabhu, P. Rao, *J. Environ. Chem. Eng.* **2013**, *1*, 676.
[46] N. K. Gupta, C. Verma, M. A. Quraishi, A. K. Mukherjee, *J. Mol. Liq.* **2016**, *215*, 47.
[47] X. Li, S. Deng, H. Fu, *Corros. Sci.* **2011**, *53*, 1529.
[48] E. A. Noor, *Mater. Chem. Phys.* **2009**, *114*, 533.
[49] T. Chen, H. Gan, Z. Chen, M. Chen, C. Fu, *J. Mol. Struct.* **2021**, *1244*, 130881.
[50] H. Cen, X. Zhang, L. Zhao, Z. Chen, X. Guo, *Corros. Sci.* **2019**, *161*, 108197.
[51] X. Li, S. Deng, N. Li, X. Xie, *J. Mater. Res. Technol.* **2017**, *6*, 158.
[52] A. Zarebidaki, A. Seifoddini, T. Rabizadeh, *J. Alloys Compd.* **2017**, *736*, 17.
[53] C. M. Fernandes, M. V. P. Mello, N. E. dos Santos, A. M. T. Souza, M. Lanznaster, E. A. Ponzio, *Mater. Corros.* **2020**, *71*, 280.
[54] M. A. Deyab, A. S. Fouda, M. M. Osman, S. Abdel-Fattah, *RSC Adv.* **2017**, *7*, 45232.
[55] J. Halambek, K. Berković, *Int. J. Electrochem. Sci.* **2012**, *7*, 8356.

[56] X. Li, S. Deng, T. Lin, X. Xie, *J. Mol. Liq.* **2019**, *282*, 499.
[57] S. Bashir, A. Thakur, H. Lgaz, I. M. Chung, A. Kumar, *Surf. Interfaces* **2020**, *20*, 100542.
[58] Z. Moghadam, M. Shabani-Nooshabadi, M. Behpour, *J. Mol. Liq.* **2017**, *242*, 971.
[59] H. S. Mandour, A. A. Nazeer, E. Al-Hetlani, M. Madkour, Y. K. Abdel-Monem, *New J. Chem.* **2018**, *42*, 5914.

How to cite this article: T. Rabizadeh, A. Matin Javid, M. Kazemi, N. Vahedian Khezerlou, H. Ghanbari, *Mater. Corros.* **2023**, *74*, 1521–1534. https://doi.org/10.1002/maco.202313909